JOURNAL OF MATERIALS SCIENCE: MATERIALS IN MEDICINE 13 (2002) 175–184

Production of thin calcium phosphate coatings from glass source materials

J.D. HAMAN[1]*, R.N. SCRIPA[2], J.M. RIGSBEE[3], L.C. LUCAS[1]
[1]Department of Biomedical Engineering, University of Alabama at Birmingham, 1075 13th Street South, Birmingham, Alabama, 35294-4440
[2]Department of Materials and Mechanical Engineering, University of Alabama at Birmingham, 1150 10th Avenue South, Birmingham, Alabama, 35294-4440
[3]Department of Materials Science and Engineering, North Carolina State University, Raleigh, North Carolina, 27695-7907

Calcium phosphate (CaP) coatings, from 40 000 to 200 000 nm thick, on titanium and titanium alloy substrates, were produced using radio frequency (RF) sputtering. Such coatings on dental implants have the potential for improving initial bone ingrowth rates. The success of these coatings may allow the movement from two stage implant systems to single stage implant systems, significantly reducing the time required for healing and fixture placement. Glass source materials were developed for the RF sputtering facility and the resultant coatings were characterized and compared to coatings sputtered from a conventional plasma sprayed hydroxyapatite (HA) source material. The coatings were characterized according to their chemistry, crystalline orientation, and residual strain.

1. Introduction

In 1983, Brånemark published a review article on the osteointegration of commercially pure titanium dental implants [1]. Brånemark detailed studies which led to the use of two stage dental implants, where the first stage is implant placement and the second stage is fixture placement and loading. Radiographic evidence indicated that bone density in the immediate vicinity of the successful implant increased with time, leading Brånemark to the conclusion that a successive load-adapted bone remodeling was taking place in the interface region. However, he also determined that implants might be lost as a result of three primary mechanisms:

- Soft tissue encapsulation during initial healing;
- Repeated overloading;
- Bone anchorage loss due to gradual migration of the marginal bone level toward the apex of the implant [2].

Although Brånemark and co-workers were able to show excellent results for the osteointegration of their dental implants, the same success rates have not been observed universally for all dental and orthopedic implants. In the years following Brånemark's report [1], a multiplicity of implant designs and materials have been developed, with varying degrees of success or failure. The exact mechanism responsible for success or failure of an implant is not always apparent. For example, hydroxyapatite (HA) in the bulk form is successfully used for filling of maxillofacial defects [3–5]. However, due to its poor mechanical properties, use of this form of HA in a loaded situation is not recommended [6]. In order to make use of its osteoconductive nature in a loaded bony environment, relatively thick, plasma sprayed HA coatings were developed which could take advantage of the mechanical strength of the underlying material (most often commercially pure (c.p.) titanium or Ti-6Al-4V [7–10]. In coating form, however, the success or failure of the material is not easily predicted [11].

Plasma sprayed calcium phosphate (CaP) coatings have been plagued with manufacturing difficulties such as lack of mechanical integrity within the coating, lack of coating to substrate bond strength, inconsistent levels of crystalline content, inconsistency in calcium phosphate phases produced, and inclusion of process induced impurities [11]; with these difficulties varying between manufacturers [12, 13]. On the other hand, these problems are not necessarily detrimental to the success of the implant. The true interactions that enable HA and other calcium phosphate phases to respond well to implantation are not well known. Experimental and clinical results vary widely, possibly due to these manufacturing difficulties, leading to controversies over the appropriate level of crystalline content and rate of dissolution [14–17]. Also, given the osteointegrating behavior of c.p. Ti and Ti-6Al-4V, the question has arisen as to the need for long term coating stability [18].

*Author to whom all correspondence should be addressed.

In vitro and *in vivo* studies of different CaP coatings and bulk materials have shown that early osteointegration (as compared to c.p. Ti implants) can be achieved despite various dissolution rates and mechanisms [14, 19]. Most of these studies have not attempted to explain the cause of this cellular and tissue behavior. As a result, one question which needs to be answered is: what causes the bone cells to mineralize in response to the presence of CaP implants? To begin to answer this question, coating materials must be made which have known and consistent physical and chemical properties. Thus, the objective of this research project was to produce a series of CaP coatings with known but varying crystal structure and residual strain, which can subsequently be used to systematically evaluate dissolution and *in vivo* behavior. RF magnetron sputtering was chosen to enable control of the resultant coating's crystal structure and residual strain as reported by Jansen *et al*. [20]. Coatings were produced from different source materials. One source material was plasma sprayed HA similar to that used by Jansen *et al*. [20] and the other source material was CaP glasses produced by melting appropriate CaP materials.

2. Materials

The plasma sprayed HA source materials were generously provided by Praxair Thermal Technologies. HA was applied to a 3 in copper disk by a Mach II plasma spray system (Praxair Thermal Technologies, Appleton, Wisconsin, USA) using the following conditions: 10.16 cm stand-off distance, 3048 cm/min sample traverse speed, 0.3175 cm pitch, Argon arc gas, Helium secondary arc gas, and Argon carrier gas.

For the preparation of the glass source materials, CaP, monobasic, monohydrate ($Ca(H_2PO_4)_2 \cdot H_2O$) crystals (Baker) were melted in either a 200 mL fused silica crucible (Fisher) or a 350 mL platinum crucible and subsequently poured into a graphite mold. A titanium mesh (grade 1) was used in some of the glass source materials to improve stability during the sputtering procedure. Coatings were applied to either Ti-6Al-4V-ELI (grade 5) or c.p. Ti (grade 2) disks, 0.635 cm in diameter, which were ground using 60–800 grit silicon carbide and polished using 5 and 0.3 μ alumina powders.

3. Methods

3.1. Production of calcium phosphate glass source materials

Approximately 110 g of CaP was placed in either platinum or fused silica crucibles. The crucible was placed in a resistively heated furnace and the temperature was increased to 600 °C and was held for 6 h to drive off volatiles. This was followed by heating at a rate of 120 °C/h to 1200 °C. The melt was held at 1200 °C for 4–17 h to vary the quantity of silica incorporated from the silica crucible into the final glass. The resulting glass was poured into a pre-heated graphite mold which was subsequently placed into a 450 °C furnace for 4 h followed by furnace cooling to room temperature.

3.2. Production of calcium phosphate coatings

All coatings were produced under an argon pressure of 5 mTorr with a rotating substrate holder. The power level of the RF magnetron sputtering system was set at 600 W for the plasma sprayed HA source material, as determined from previously reported studies [20]. For the glass source materials, pilot studies were performed in which the power level was increased from 200 W to 450 W in 50 W increments. Transmission electron microscopy (TEM) analysis was used to evaluate the presence of microcrystallinity and coating thickness analysis was used to determine coating efficiency.

3.3. Analytical techniques

Fourier transform infrared spectroscopy (FTIR) was used to determine the molecular composition of the starting calcium phosphates, source materials, and coatings. For calcium phosphates and the source materials, triplicate samples of a 1 : 99 weight ratio of powdered samples to potassium bromide was prepared for each analysis. A Mattson Research Series FTIR Spectrometer (Mattson Instruments, Madison, Wisconsin, USA) with a Spectra Tech diffuse reflectance accessory was used for these studies. FTIR analyses of the coatings were performed using a Spectra Tech Analytical Microscope (Spectra Tech, Madison, Wisconsin, USA) in reflectance mode. The parameters used for the powder studies were as follows: 4000–500 cm^{-1} range, 4 cm^{-1} resolution, and a gain of 4. Spectra were produced by the collection and co-adding of 1000–5000 scans. Parameters for the coating studies were similar to those for the powdered materials, with changes only to the range (lower limit of 700 cm^{-1}) and resolution (16 cm^{-1}) due to the differing capabilities of the microscope. Deconvolution and curve-fitting were performed with Grams32 (Galactic Industries Corp., Salem, New Hampshire, USA) to determine the CaP phases present in the starting powders and coatings.

Thin film X-ray diffraction (TFXRD) was used to determine the crystal structure and phases present in the coatings. A Philips X'Pert diffractometer (Philips Analytical, Natick, Massachusetts, USA) was used at the following settings: 45 KeV, 40 mA, 0.04° 2θ step size, and a 10 s scan time increment in thin film mode (0.25° or 1° θ). Alignment of the diffracting surface with the goniometer was confirmed with a dial gauge probe that was accurate to ± 1 μm. The studies were performed over a 10–60° 2θ range using a CuK_α radiation source with a wavelength of $\lambda = 1.5412$ Å. Data obtained from these analyses were used to determine the presence of HA, the presence of other calcium phosphate phases, and the crystalline structure of the coating, i.e. any preferred orientation or residual strain present. A qualitative comparison of the relative crystal size, relative preferred orientation, and relative residual strain of the different coatings was performed. A qualitative estimate of each coating's relative crystal size was determined by comparing the full width at half-maximum height (FWHM) of the (0 0 2) peak [21]. The presence of preferred orientation of the crystal structure was determined by noting deviations in peak height from

standard HA (ICDD file 9-0432) for (0 0 2) and (2 1 1) peaks [21]. A qualitative estimate of residual strain was determined from peak position shifts, with larger shifts signifying larger residual strain [21].

Profilometry was used to determine coating thickness. An Alpha-Step 500 Surface Profiler (KLA Tencor Corporation, San Jose, California, USA) was used with the following parameters: scan length of 5000 μm, speed of 0.5 μm/s and a stylus force of approximately 13 mg. Thickness tests were performed on glass substrates that were partially masked during coating deposition. After coating, the masking was removed and the height (or thickness) of the coating was determined by scanning from the masked to the unmasked areas [22].

The silica and total phosphate concentration of the glass source materials was determined through the formation of a vanadomolybdate complex that was analyzed spectrophotometrically on a Shimadzu UV160U UV-Vis spectrophotometer (Shimadzu Scientific Instruments, Inc., Columbia, Maryland, USA). A Perkin-Elmer 3030B flame atomic absorption spectrophotometer (PerkinElmer, Inc., Norwalk, Connecticut, USA) was used to determine the calcium content of the source materials and coatings (removed by a 5%–10% hydrochloric acid solution). Linear calibration curves were generated for silica, calcium, and phosphates. AA and UV-Vis analytical methods for these materials have been described previously by several investigators [23–25].

All studies were performed in triplicate, or greater, as required for statistical significance.

4. Results and discussion

4.1. Glass source material development

Most RF sputtering of CaP coatings is performed with a plasma sprayed CaP source material. Several researchers [20, 26, 27] have been able to produce crystalline coatings exhibiting imperfect crystalline structures (texture, residual strain) during sputtering alone, necessitating post-deposition heat treatments to increase crystal structure perfection. An extensive study in this area was performed by van Dijk *et al*. [28]. It was also shown by Yamashita *et al*. [29], that a CaP glass source material could produce amorphous CaP coatings that could then be transformed into crystalline coatings through post-deposition heat treatments. These coatings, in combination with those produced from plasma sprayed hydroxyapatite source materials, would then allow the determination of the effects of texture and residual strain on subsequent dissolution and *in vivo* studies. Therefore, in this study, we developed and optimized a glass source material made from the melt of CaP monobasic, monohydrate crystals.

During initial experiments, ingots of glass were produced from the melting of CaP monobasic, monohydrate in fused silica crucibles. Table I lists the melt times and resulting compositions (determined as described above) for each melt time. Due to the use of fused silica crucibles, the longer melt times led to undesirable concentrations of silicon (Si) in the glasses. Thus, shorter melt times and ramp rates were investigated. It was determined that a 2 h melt time with a step up to 600 °C and a rate of 120 °C/h to 1200 °C would provide adequate viscosity of the molten glass and a low silicon content. It is worth noting that silicon can cause a major interference when quantifying phosphates by methods such as UV-Vis spectroscopy [25]. Therefore, a molybdate blue method which would limit this interference was chosen for determining the concentration of phosphates in these [25]. However, as can be seen in Table I, the concentration of phosphates increased with increasing melt time, indicating that the silicon interference was still occurring. Normally, it would be expected that phosphate concentrations would decrease with increased time only at extreme temperatures. For example, as a result of processing parameters plasma sprayed coatings have lower phosphate concentrations (molar Ca : P of up to 2, as opposed to 1.67 for HA [12]) than their starting materials. Therefore, a short melt time is beneficial not only in reducing the silicon content of the material, but also reducing its ability to interfere with phosphate determinations. In an attempt to eliminate the silicon content, a platinum crucible was used. However, source materials poured from platinum crucibles tended to crystallize during the sputtering process, leading to deposition of undesirable CaP phases.

TABLE I Calcium (Ca), Phosphorous (P), and Silicon (Si) concentrations (in wt %) of glass ingots

Melt Times	[Ca]	[P]	[Ca]/[P]	[Si]
4 h	17.21	9.52	1.81	0.433
8 h	17.70	10.36	1.71	0.559
12 h	17.41	11.65	1.49	0.689
17 h	17.91	13.51	1.33	3.99

During the early to mid 1990s several studies were reported in which the addition of small amounts of silicon into the crystal lattice of hydroxyapatite bulk ceramics was attempted [30–35] under the hypothesis that this would lead to bioactivity similar to that of bioactive glasses [36]. It is well documented that rapid reactions at the surface of silicate-based bioactive glasses lead to interfacial bonding between the glasses and the tissues *in vivo* [36]. This hypothesis was in part the result of *in vitro* and *in vivo* bone calcification work performed in the late 1960s and through the 1970s by Carlisle [37, 38], in which evidence from electron microprobe analyses showed up to 0.5 wt % silicon to be localized in active bone growth areas in young mice. Therefore, the possible addition of silicon to the CaP coating structure via its presence in the glass source materials may not be of concern, and, in fact, may be beneficial.

4.2. Coating parameter studies for glass source materials

Coating efficiency (coating thickness divided by coating time), scanning electron microscopy (SEM), and transmission electron microscopy (TEM) studies were used to determine the most appropriate RF magnetron parameters for use with the glass source materials. For the TEM studies, special substrates were used: specimen grids (copper, 150 mesh) with pure carbon support films deposited onto one side. Other substrates used in this

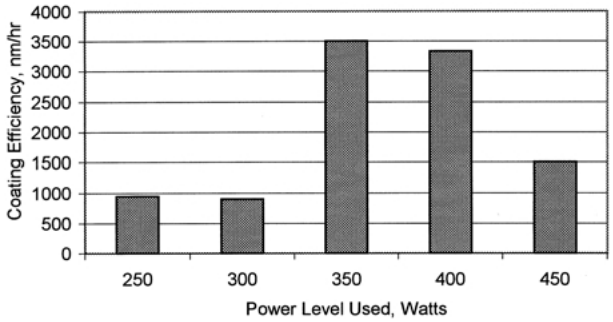

Figure 1 Coating efficiency (coating thickness divided by coating time).

series of studies included c.p. Ti disks, Ti-6Al-4V disks, and glass slides. The substrates were coated at 250, 300, 350, 400, and 450 W.

The coating efficiency was determined by dividing the thickness of the coatings by coating time. As seen in Fig. 1, the coating efficiency generally increased as the wattage used to coat increased. However, beginning at 400 W, and even more so at 450 W, the trend reversed itself, and coating efficiency decreased with increased wattage. This non-linearity may be due to the electrical conduction properties of the glass. A mechanism analogous to space-charge limited (SCL) conduction may be occurring. Briefly, in SCL, non-linear conduction behavior is a result of exceeding the rate at which charge can be transported through the material [22]. Although not shown in Fig. 1, it was also noted that coating efficiency decreased with continued use of the source material.

Early SEM studies showed as-sputtered coatings on c.p. Ti produced at high wattages (500–600 W) contained bubbles (Fig. 2). These were hypothesized to be caused by either outgassing of the substrate or excessive heating of the coating during the coating process. Therefore, three routes were taken concurrently to reduce the occurrence of the bubbles. First, the power levels were kept at a moderate level to avoid excessive heating. Second, the substrates (c.p. Ti and Ti-6Al-4V) were not passivated (typically performed on titanium for implants to thicken the oxide layer [39]) prior to coating to avoid

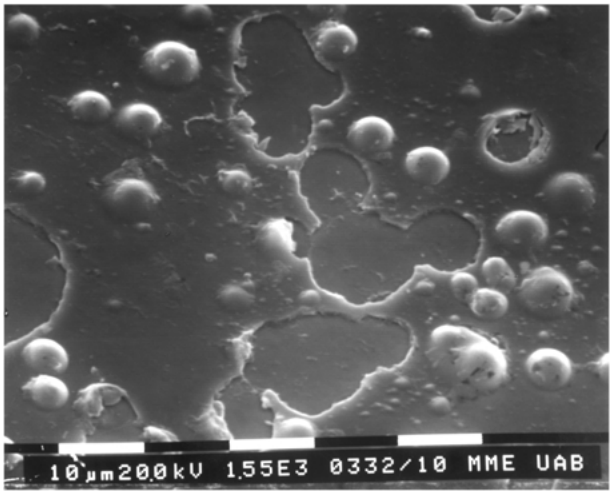

Figure 2 Bubbles in as-sputtered coatings from glass target (bar is 10 µ) thought to result from out-gassing of the substrate during deposition.

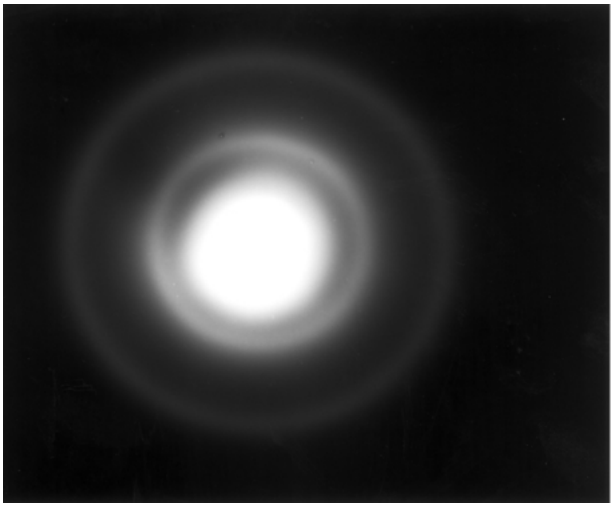

Figure 3 Electron diffraction of 250 W as-sputtered coating – an example of the amorphous nature of the majority of the as-sputtered coatings from the glass source material.

N_2 adsorption and subsequent outgassing. Finally, on the slight chance that the bubbles might be caused by gasses trapped within the metal substrates, a pre-polish, pre-deposition heat-treatment at 875 °C in vacuum for 24 h was performed on the Ti substrates.

Additionally, due to the thermal expansion properties of the glass source materials, thermal shock of the source was found to be a significant problem. Thermal shock was avoided by using a very slow rate (1 W/min) of wattage increase to the appropriate coating level, followed by a slow rate back down. In later experiments, source materials were made by pouring the melted glass over a titanium mesh (grade 1, 8 × 8 mesh, Belleville Wire Cloth Co., Inc.) to hold the glass together in the event of thermal shock.

On the hypothesis that nanocrystallinity would provide seed material for crystal formation during subsequent heat treatments of the coatings, TEM and electron diffraction was used to determine if nanocrystallinity was present in the as-sputtered coatings. Most of the coatings were completely amorphous as indicated by the diffuse electron diffraction ring pattern in Fig. 3. However, the presence of sharper rings in the coatings produced at 300 W (Fig. 4) indicated that nanocrystals may have been present.

The results of the coating efficiency, SEM and TEM studies indicate that the best overall coating is one produced at 300 W. This is a result of compromises made between coating efficiency, source material thermal shock constraints, increased time and equipment costs associated with the thermal shock properties, the presence of nanocrystals at this wattage, and finally, reduced process induced outgassing of the substrates and subsequent bubbling of the coatings.

4.3. DTA studies of glass source materials

Since the coatings were primarily amorphous, the temperature at which any phase changes occurred had to be determined in order to select appropriate post-deposition heat-treatment temperatures for subsequent crystallization. Differential thermal analysis (DTA) of

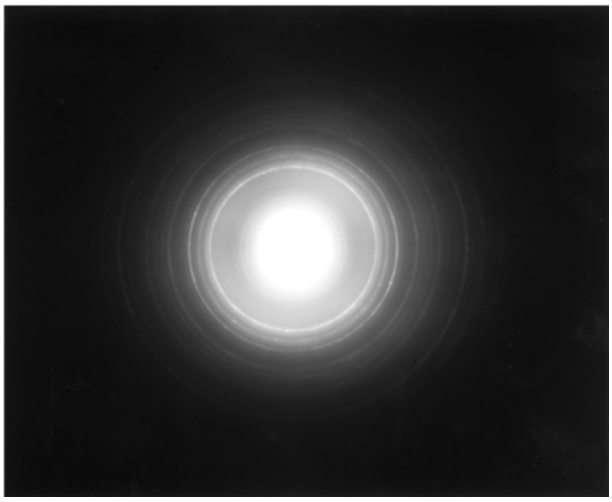

Figure 4 Electron diffraction of 300 W as-sputtered coating, which is thought to contain nanocrystallinity as a result of the somewhat sharper definition of the rings as compared to Fig. 3.

the coatings is highly difficult due to the small amount of material involved, thus, the glass source materials were used to evaluate phase-change temperatures. It is reasonable to assume that the composition of the coatings and the glass source materials are essentially the same. DTA analysis was carried out at heating rates of 5 and 2 °C/min in an inert atmosphere (argon or nitrogen). Several samples from different source materials were used. Four events were observed at temperatures of 550, 620, 705, and 925 °C (Fig. 5). Therefore, these temperatures were used in subsequent post-deposition heat-treatment studies to evaluate the optimum temperature to produce the desired crystalline structure.

4.4. Heat treatment studies

For the heat-treatment studies, coatings were applied at 300 W to both c.p. Ti and Ti-6Al-4V substrate disks. Heat-treatments were performed at 550, 620, 705, and 925 °C. All heat-treatments on coatings made from glass source materials were carried out for up to 24 h, in a water saturated argon atmosphere. The furnace was brought up to temperature at no more than 5 °C/min and cooling occurred either as the furnace naturally cooled or at a controlled rate of no more than 2 °C/min. At least three substrates of each material were heat-treated at each temperature. The coatings were then analyzed by TFXRD and FTIR to determine the phases formed at each temperature.

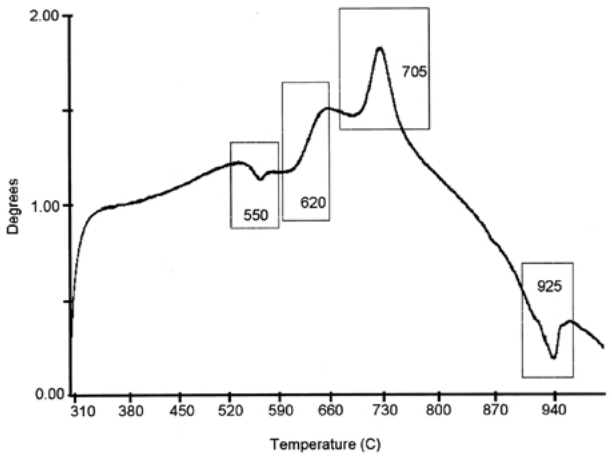

Figure 5 Example DTA results from glass source materials. DTA parameters included a 5 °C/min heating rate and nitrogen atmosphere. DTA results are plotted as change in temperature (degrees) vs. temperature. Boxed areas of the curve indicate features of interest. At 550 °C and 925 °C, an endothermic reaction occurs, indicated by a valley. At approximately 620 °C, a change in slope occurred. At 705 °C a relatively large exothermic reaction occurred.

An overview of the chemistries and crystalline structures formed as a result of the post-deposition heat-treatments can be seen in Table II. No significant crystallization was apparent in coatings heat-treated at 550 °C, and FTIR analysis showed that the coatings were very similar to the as-sputtered coatings that were amorphous calcium phosphate (ACP). However at 620 °C, TFXRD revealed a mix of highly textured (oriented) HA and tetracalcium phosphate (TTCP) crystal structures. At 705 °C, an HA crystal structure with no evident texturing (random orientation) and possible trace contaminations of TTCP and carbonated apatite was found. Finally, coatings heat-treated at 925 °C were found to consist of calcium titanate. Fig. 6 contains sample diffractograms and FTIR spectra from each heat-treatment temperature studied.

Although no differences in the phases present in the coatings between the two substrate materials were noted for any temperature, coatings on c.p. Ti exhibited failures due to the introduction of excessive compressive strain [22]. Coatings on Ti-6Al-4V did not exhibit this tendency. This was attributed to a difference in the thermal expansion coefficient of the two substrate materials. Additionally, coatings that underwent post-deposition heat-treatments at 925 °C lacked adherence to the substrates, flaking (or spalling) off quite easily, for both c.p. Ti and Ti-6Al-4V substrates.

4.5. Analysis of coatings from plasma sprayed source materials

Coatings made from plasma-sprayed source materials were deposited at 600 W [20], onto c.p. Ti disks. Post-deposition heat treatments performed at 550 °C for 2 h [40] (with a 5 °C/min heating rate and a 0.5 °C/min cooling rate) resulted in hydroxyapatite coatings with lower residual strains and possible smaller crystal size compared to the as-sputtered coatings (Table III). No change in coating chemistry (i.e., phases present) was expected or seen as a result of the post-deposition heat-treatment. However, FTIR data indicated the presence of

TABLE II Coatings obtained based on post-deposition heat-treatment

Heat treatment	Major phase in coating
None	Amorphous calcium phosphate (ACP)
550 °C, 24 h	ACP
620 °C, 24 h	Tetracalcium phosphate (TTCP) (with traces of textured HA)
705 °C, 6 h	HA, randomly oriented crystals (with traces of TTCP)
925 °C, 24 h	Calcium titanate

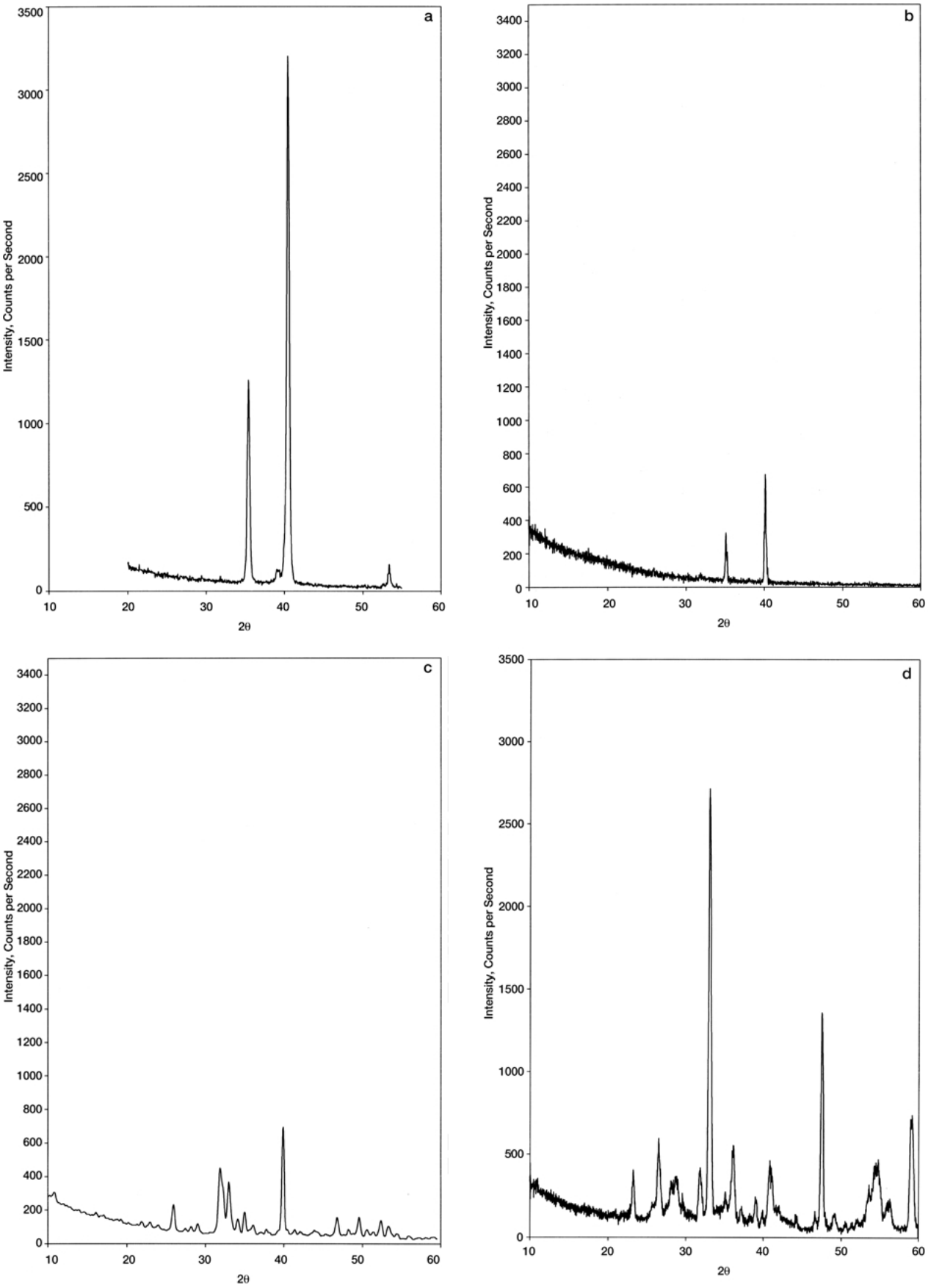

Figure 6 TFXRD and FTIR of post deposition heat-treated coatings from glass source materials. TFXRD: a, 550 °C; b, 620 °C; c, 705 °C; d, 925 °C. FTIR: e, 550 °C; f, 620°; g, 705 °C; h, 925 °C.

carbonate species (single band around 1400 cm^{-1}) after the heat treatment. It was hypothesized that these carbonates were likely surface molecules adsorbed but not incorporated into the bulk of the coating as a result of the relatively short heat treatment. A depth profiling analytical technique such as Auger electron spectroscopy (AES) or X-ray photoelectron spectroscopy (XPS) could be used to prove this hypothesis. No change in coating

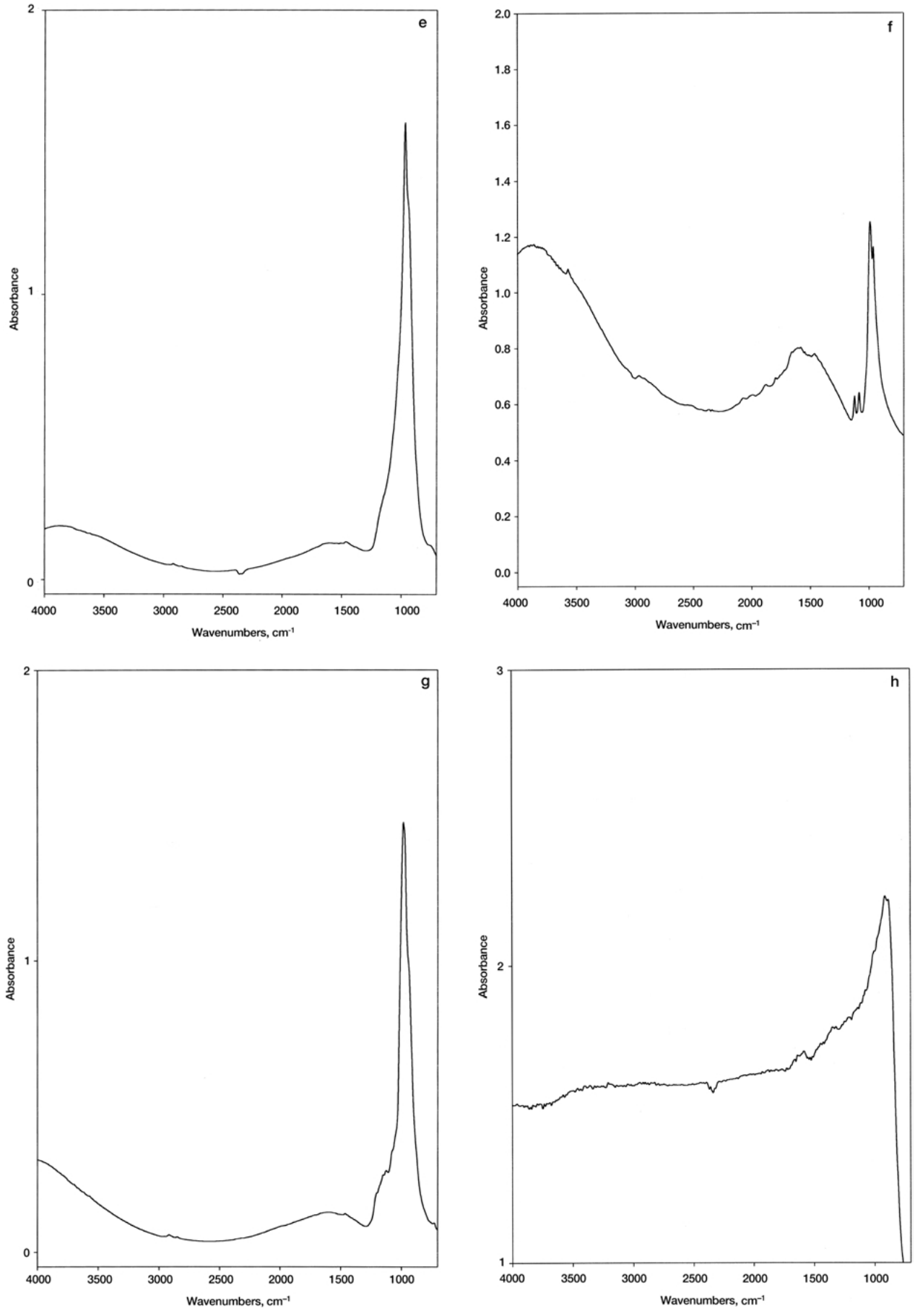

Figure 6 (Continued)

texture or orientation was noted (Table III). Evidence of the lack of changes can be seen in XRD diffractograms and FTIR spectra for these coatings (Fig. 7).

Because residual strain can be seen in XRD data as both peak shifts and/or peak broadening (resulting from uniform or non-uniform strain, respectively), and crystal

TABLE III Diffraction data from HA coatings from plasma sprayed source material

Post-deposition heat treatment	Coating material	Crystal orientation (relative intensity of peak)	Peak width (0 0 2) (indication of crystal size/ non-uniform strain)	Average peak shifts from ICDD 9-432 (indication of uniform residual strain)
None	HA, textured, strained crystals	(2 1 1) = 0% (0 0 2) = 100%	0.32409 ± 0.00031	0.5°2θ lower
550 °C	HA, textured crystals	(2 1 1) = 0% (0 0 2) = 82%	0.4733 ± 0.000086	0.05°2θ lower

size is normally determined through peak breadth measurements, differentiating between strain and crystal size changes can be difficult with XRD data alone [21]. The peak shifts (compared to ICDD standards for HA powders) seen in the as-deposited coatings indicate residual strain was present in these coatings. Said strain, however, could be a product of residual thermal stresses or large interstitial substitution atoms [21]. As with the carbonates seen in the heat-treated coatings, the exact cause of the strain could be determined with the aid of AES or XPS studies. In the absence of these studies; however, the reduction of the peak-shifts seen after the heat-treatment led to the hypothesis that the strain was a result of residual thermal stresses, which were relieved by the heat-treatment. Finally, the literature supports the hypothesis that the peak shifts seen in the as-sputtered coatings are strain. Often noted with sputtered thin films, residual thermal strains are a result of a mismatch between the thermal coefficient of expansion of the coating and the substrate [20, 26, 27]. Additionally, strains may result from misfit produced by epitaxial growth of the crystalline coating during the sputtering process [22].

However, as stated above, the width of the peaks can be attributed to both residual strain and crystal size [21]. Heat-treatment reduced the uniform residual strain in the coatings, as seen by the significantly lower peak-shifts. The peaks were also seen to broaden in comparison to the as-deposited coatings, indicating a decrease in crystal size. This broadening may also indicate the presence of non-uniform residual strains [21]. However, it was hypothesized that the evidence of residual strain and preferred orientation in the as-sputtered coatings would provide enough thermodynamic energy for recrystallization to take place during the post-deposition heat-treatment, even though the coatings were exposed to the heat-treatment for a relatively short time. Additionally, the extremely slow cooling rate used (0.5 °C/min) would have allowed the samples to be at the higher temperatures for a longer period, allowing even more time for recrystallization to occur. As further evidence of the presence of smaller crystal sizes in the heat-treated coatings, in separate but concurrent atomic force microscopy studies of these materials, a qualitative decrease in feature size to approximately one third that of the as-sputtered coatings was seen [40].

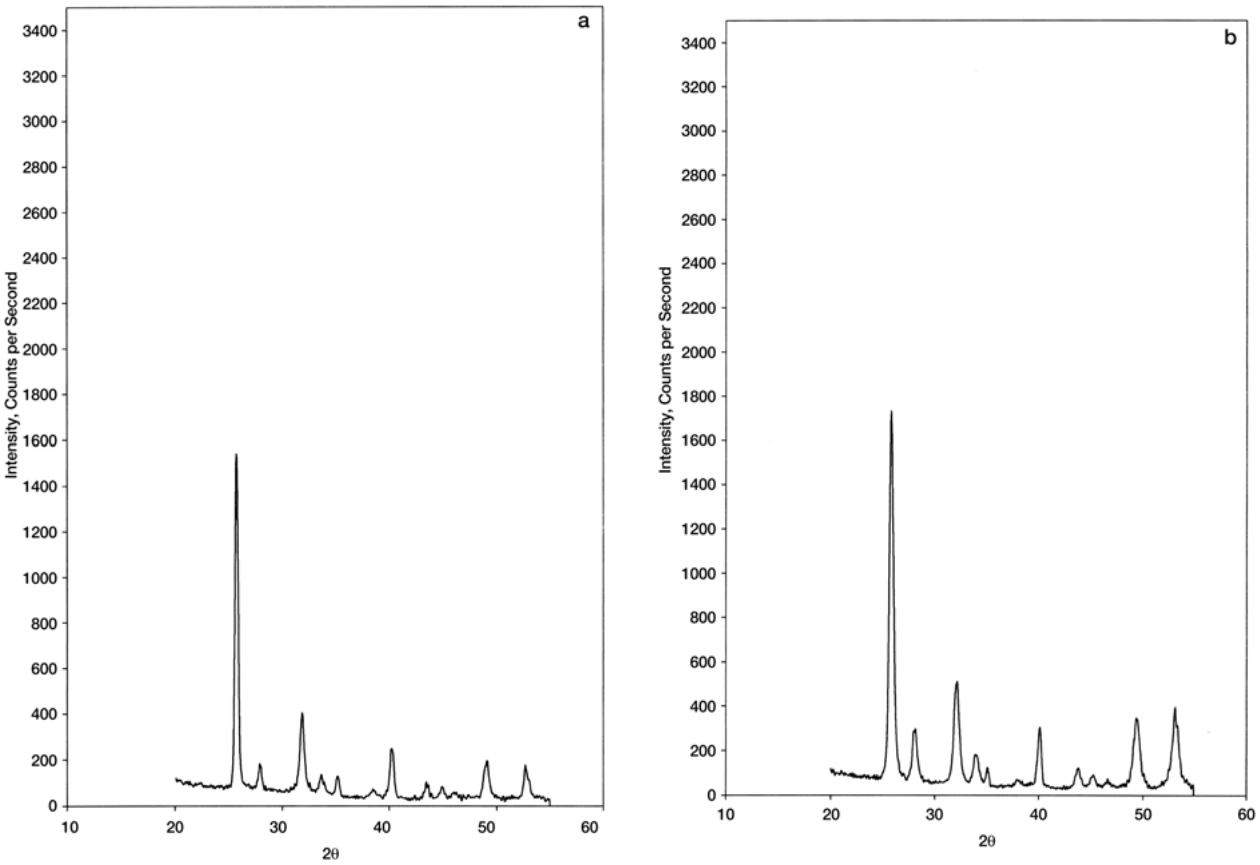

Figure 7 Sample TFXRD and FTIR of coatings from plasma sprayed source material. TFXRD: a, as-sputtered; b, heat treated at 550 °C. FTIR: c, as-sputtered; d, heat treated at 550 °C.

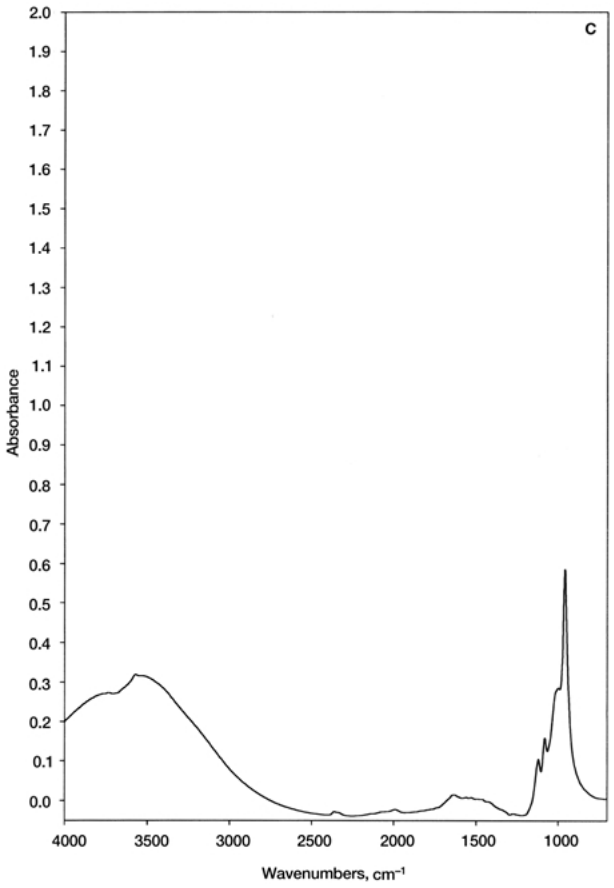

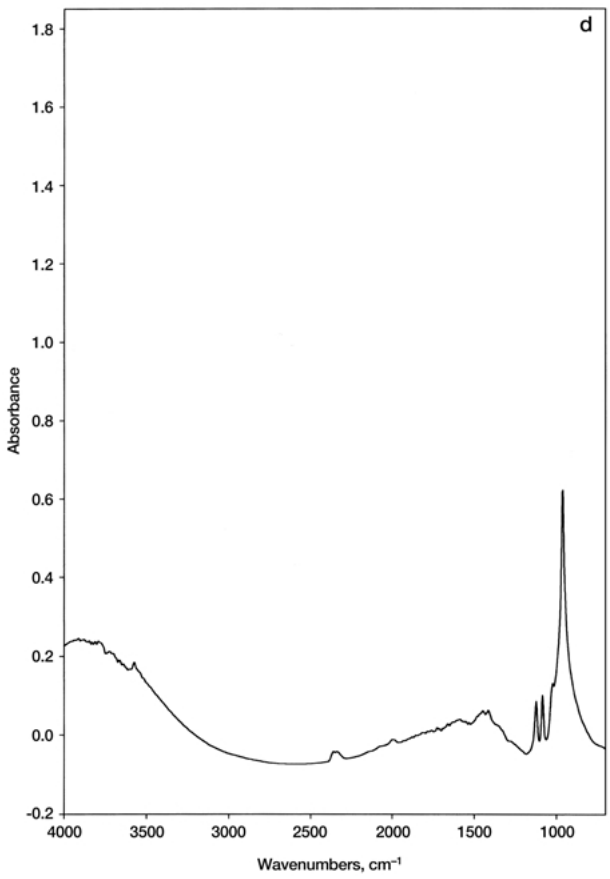

Figure 7 (Continued)

Taking into consideration all of the CaP materials produced in this study, the hydroxyapatite coatings prepared from glass and plasma sprayed target materials were chosen for future investigations due to the numerous studies available for comparison to bulk hydroxyapatite dissolution characteristics. The hydroxyapatite coatings developed and described here should provide reproducible dissolution behavior, allowing the description of mechanism of dissolution to be determined based on controllable factors such as internal strain, chemistry, and roughness. Consequently, prediction of the behavior of these coatings *in vivo* will be more easily accomplished.

5. Conclusions

The objective of this research was to produce a series of CaP coatings with known but varying crystal structures and residual strains. To that end, the following can be stated:

- Calcium phosphate glass materials were successfully developed for use as source materials in an RF sputtering system.
- Coating deposition and post-deposition heat-treatment parameters were optimized for the successful production of randomly oriented hydroxyapatite coatings from the glass source materials.
- Plasma sprayed hydroxyapatite source materials were used in the RF sputtering system to produce strained, textured, hydroxyapatite coatings; and post-deposition heat-treatments were used to reduce the residual strain and crystal size of these coatings.

Acknowledgments

The authors thank Drs Vohra Yogesh, Aaron Catledge, and Mary Ellen Zvanut of the Department of Physics at the University of Alabama at Birmingham for XRD and profilometry instrument use. DTA instrument and furnace equipment use was kindly provided by Drs Robin Griffin and Gregg Janowski in the Department of Materials and Mechanical Engineering, University of Alabama at Birmingham. Additional thanks go to the Whitaker Foundation and the National Science Foundation (EPS 9720157) for financial support of this research.

References

1. P. I. BRÅNEMARK, *J. Pros. Dent.* **50** (1983) 399.
2. P. I. BRÅNEMARK, R. ADELL, T. ALBREKTSSON *et al., Biomat.* **4** (1983) 25.
3. J. W. FRAME and C. L. BRADY, *Brit. J. Oral & Maxillofac. Surg.* **25** (1987) 452.
4. C. ZELTSER, R. MASELLA, J. CHOLEWA *et al., J. Pros. Dent.* **62** (1989) 441.
5. B. SHIPMAN, I. M. FINGER and L. R. GUERRA, *Adv. Ophthal. Plas. & Reconst. Surg.* **9** (1992) 297.
6. S. D. COOK and J. E. DALTON, *Alp. Om.* **85** (1992) 41.
7. K. SOBALLE, *Acta. Ortho. Scand. Supp.* **255** (1993) 1.
8. T. S. GOLEC and J. T. KRAUSER, *Dent. Clin. N. Am.* **36** (1992) 39.

9. S. D. COOK, K. A. THOMAS, J. F. KAY *et al*., *Clin. Ortho. & Rel. Res.* **232** (1988) 225.
10. G. SAUER, *Biomed. Technik.* **33** (1988–) 300.
11. A. R. BIESBROCK and M. EDGERTON, *Int. J. Oral. Maxillofac. Imp.* **10** (1995) 712.
12. J. D. BUMGARDNER, M. D. ROACH, S. D. GARDNER and J. L. ONG, in ''Transactions from the 25th Annual Meeting of the Society For Biomaterials'', Providence, 1999, p. 164.
13. R. Z. LEGEROS, *Mono. Oral Sci.* **15** (1991) 1.
14. E. B. NERY, R. Z. LEGEROS, K. L. LYNCH *et al., J. Perio.* **63** (1992) 729.
15. R. Z. LEGEROS and R. G. CRAIG, *J. Bone Min. Res.* **8** (Suppl 2) (1993) S583.
16. S. H. MAXIAN, J. P. ZAWADSKY and M. G. DUNN, *J. Biomed. Mater. Res* 27(1) (1993) 111–117.
17. S. R. RADIN and P. DUCHEYNE, *ibid.* **27** (1993) 35.
18. W. C. HEAD, D. J. BAUK and R. H. EMERSON, JR., *Clin. Ortho. Rel. Res.* **311** (1995) 85.
19. R. Z. LEGEROS, J. R. PARSONS and G. DACULSI *et al*., *Ann. New York Acad. Sci.* **523** (1988) 268.
20. J. A. JANSEN, J. G. WOLKE, S. SWANN, J. P. VAN DER WAERDEN and K. DE GROOT, *Clin. Oral Im. Res.* **4** (1993) 28.
21. B. D. CULLITY, in ''Elements of X-ray Diffraction'' (Addison-Wesley Publishing Company Inc., Reading, Massachusetts, 1978).
22. M. OHRING, in ''The Materials Science of Thin Films'' (Academic Press, San Diego, 1991) p. 252.
23. R. K. ILER, in ''The Chemistry of Silica'' (John Wiley & Sons Inc., New York, 1979) p. 98.
24. J. D. HAMAN, L. C. LUCAS and D. CRAWMER, *Biomat.* **16** (1995) 229.
25. ASTM D 518-88 Standard test methods for phosphorus in water.
26. S.-J. DING, C.-P. JU and J.-H. C. LIN, *J. Biomed. Mater. Res.* **47** (1999) 551.
27. K. VAN DIJK, H. G. SCHAEKEN, J. G. C. WOLKE, C. H. M. MAREE, F. H. P. M. HABRAKEN, J. VERHOEVEN and J. A. JANSEN, *ibid.* **29** (1995) 269.
28. K. VAN DIJK, H. G. SCHAEKEN, J. G. C. WOLKE and J. A. JANSEN, *Biomat.* **17** (1996) 405.
29. K. YAMASHITA, T. ARASHI, K. KITASAKI, S. YAMADA and T. UMEGAKI, *J. Am. Ceram. Soc.* **77** (1994) 2401.
30. I. R. GIBSON, S. M. BEST and W. BONFIELD, *J. Biomed. Mater. Res.* **44** (1999) 422.
31. A. J. RUYS, *J. Aust. Ceram. Soc.* **29** (1993) 71.
32. Y. TANIZAWA and T. SUZUKI, *Phos. Res. Bull.* **4** (1994) 83.
33. K. SUGIYAMA, T. SUZUKI and T. SATOH, *J. Antibact. Antifung. Ag.* **23** (1995) 67.
34. L. BOYER, J. CARPENA and J. L. LACOUT, *Sol. Sta. Ion.* **95** (1997) 121.
35. K. S. LESHKIVICH and E. A. MONROE, *J. Mater. Sci.* **28** (1993) 9.
36. L. L. HENCH, *J. Am. Ceram. Soc.* **74** (1991) 1487.
37. E. M. CARLISLE, *Sci.* **167** (1970) 179.
38. E. M. CARLISLE, *Calc. Tiss. Int.* **33** (1981) 27.
39. ASTM F 86-91, Standard practice for surface preparation and marking of metallic surgical implants.
40. E. M. BURKE, J. D. HAMAN, J. J. WEIMER, A. B. CHENEY, J. M. RIGSBEE and L. C. LUCAS, Submitted to *J. Biomed. Mater. Res.* (June, 2000).

Received 15 October 2000
and accepted 13 April 2001